Methods of Suppression or Avoidance of Parallel-Plate Power Leakage from Conductor-Backed Transmission Lines

Nirod K. Das, *Member, IEEE*

Abstract— **Four useful methods are presented to suppress and/or avoid parallel-plate leakage from conductor-backed printed transmission lines. These include: 1) the use of shorting-pins; 2) the use of a dielectric-guide-coupled configuration; 3) using a two-layered conductor-backing configuration; and 4) dielectric loading on top. New analyses to model the leakage suppression due to the shorting-strips and the dielectric-guide-coupled geometries are presented, with selected demonstrative results and critical discussions. It is concluded that the unwanted leakage in many printed transmission lines, that are otherwise attractive for integrated circuits and phased array applications, can be successfully avoided and/or significantly suppressed using the proposed techniques.**

I. Introduction

THE POSSIBILITY of power leakage from the dominant mode of certain geometries of single or multilayered transmission lines is now quite well known [1]–[7]. Power leaks from such printed transmission lines in transverse directions, due to coupling to the characteristic surface-wave mode(s) of the substrate structure. The leakage can sometimes be severe for specific substrate configurations of the printed transmission lines, under certain conditions of frequency and/or physical parameters. Unfortunately, several novel geometries of printed transmission lines, which are otherwise attractive for integrated circuits and phased array applications from various practical considerations, potentially suffer from the unwanted leakage problems. For example, a conductor backing behind a standard slotline or coplanar waveguide can be attractive to achieve enhanced mechanical strength. The conductor backing would also allow additional circuit integration on its other side, providing the necessary electrical isolation in between. However, such a conductor-backed configuration, unlike a standard slotline or coplanar waveguide, can leak significant power to the parallel-plate mode, even at low frequencies [1]. This leakage can be particularly prohibitive for thin substrates and/or higher frequencies, making the conductor-backed geometries potentially dangerous to use. Similarly, a stripline with two different substrate layers (with different dielectric constants and/or thicknesses) on two sides of the central strip is attractive for a multilayer feed architecture of integrated phased arrays [8], but can be potentially leaky due to the possibility of excitation of the parallel-plate mode [3]. It is, therefore, important to investigate possible methods of suppression and/or avoidance of the unwanted leakage from useful printed transmission lines.

In this paper, we propose four possible methods of suppression and/or avoidance of leakage from a conductor-backed slotline or coplanar waveguide. Similar techniques will also be applicable for other strip- or slot-type transmission lines geometries. The proposed methods include: 1) the use of conducting shorting pins to suppress excitation of the parallel-plate mode; 2) the use of a "hybrid configuration" (as discussed later), where a small dielectric-guide" structure with a significantly high dielectric constant compared to that of the surrounding substrate, is coupled underneath the slotline or coplanar waveguide; 3) using a two-layered conductor-backing configuration, instead of the standard configurations of [1], [3] with only a single uniform substrate between the parallel plates; or 4) loading the conductor-backed geometry on top using a thin, high dielectric-constant substrate. New analyses are presented to accurately model the leakage suppression/avoidance due to the shorting strips and the dielectric-guide-coupled configurations. Important results are presented to demonstrate the success of the proposed methods. The details of the analyses of the new conductor-backed geometries are presented in Section II. Selected results for different suppression methods are presented in Section III, with discussion on the general characteristics.

II. Analysis of the New Geometries

In this section, we will separately discuss the detailed analyses of the first two geometries we have proposed. The analyses of the other two new geometries, with a dielectric cover or with a multilayer conductor backing, have been performed using the spectral-domain moment method of [9], [10], [11], and [3], and have not been duplicated in this paper. Only the results illustrating the leakage suppression are discussed in Section III.

The first geometry uses shorting pins in both sides of the central-guide region of a conductor-backed slotline or coplanar

Manuscript received December 22, 1993; revised November 12, 1995. This work was supported in part by the US Army Research Office, Research Triangle Park, NC.

The author is with the Weber Research Institute/Department of Electrical Engineering, Polytechnic University, Farmingdale, NY 11735 USA.

Publisher Item Identifier S 0018-9480(96)01437-8.

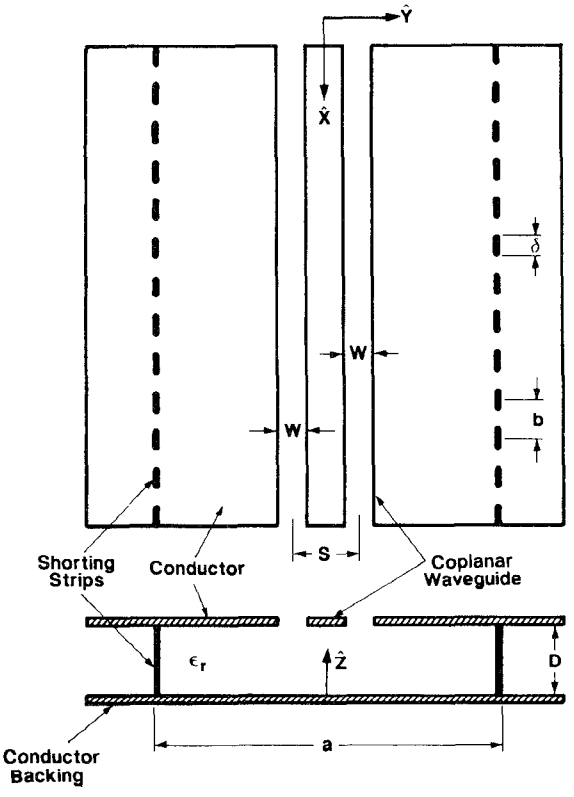

Fig. 1. Geometry of a conductor-backed coplanar waveguide with shorting-pins used to supress leakage to the parallel-plate mode A conductor-backed slotline can be obtained by replacing the dual-slots of this coplanar waveguide by a single slot of width, W, centered at $y = 0$

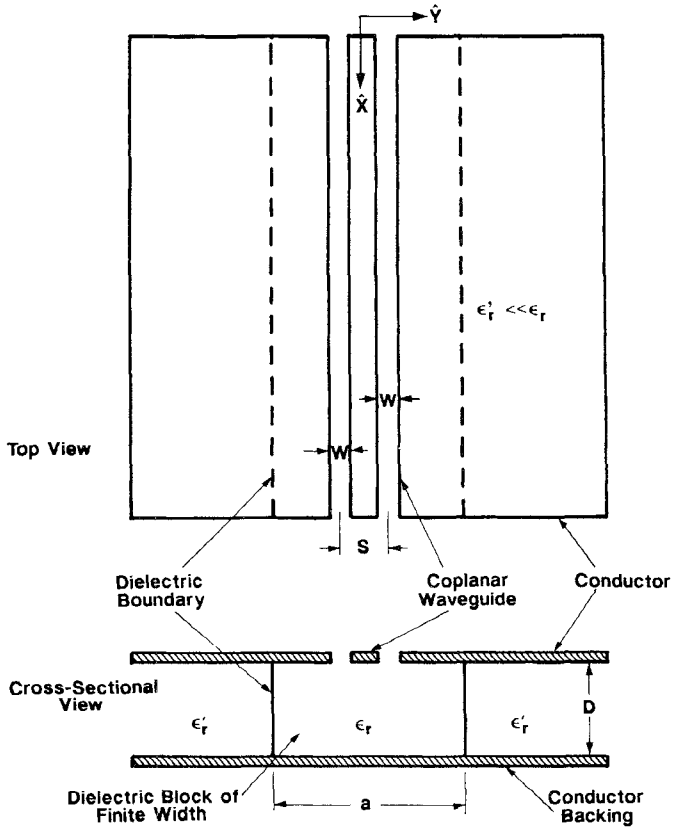

Fig. 2. Geometry of a modified conductor-backed coplanar waveguide with a finite-width dielectric guide coupled to the coplanar waveguide. A similar modified conductor-backed slotline geometry can be obtained by replacing the dual-slots of the coplanar waveguide by a single slot of width W centered at $y = 0$.

waveguide, placed periodically spaced along the propagation direction. Fig. 1 shows the geometry of a conductor-backed coplanar waveguide with "shorting strips." The shorting strips in Fig. 1 have been used for the simplicity of analytical modeling. The shorting strips would always exhibit similar characteristic trends as the shorting pins and are henceforth interchangeably referred to by one name or the other. Such shorting pins or shorting strips electrically connect the two groundplanes of the parallel-plate structure, and have been commonly used in the past by stripline designers to suppress the possible excitations of the parallel-plate mode. However, due to the nonzero gaps between the shorting strips, (b-δ) in Fig. 1, the excitation of the parallel-plate mode will not be totally eliminated. The shorting strips will only suppress the transversal leakage to the parallel-plate mode, always allowing a fraction of the power to escape through the nonzero gaps between the strips (see Fig. 1). Therefore, it is important to investigate the effects of the separation between consecutive shorting strips, b, for different strip widths, δ, and different distances, $a/2$, between the shorting strips and the center of the transmission line, on the leakage level. This would help design optimal positioning of the shorting pins, in order to suppress the power leakage to a practically acceptable low level.

The second geometry we will analyze in this section is a modified conductor-backed slotline or coplanar waveguide. Here the uniform dielectric substrate between the parallel plates of a standard conductor-based configuration is replaced by a nonuniform dielectric structure, as shown in Fig. 2. A dielectric block of finite width, a is fabricated under the central slotline or coplanar waveguide. The dielectric constant of this dielectric block, ϵ_r, should be much larger than the surrounding dielectric medium, ϵ'_r. The leakage power from the central transmission line, propagating in transverse (y) directions, gets totally reflected from the dielectric boundaries on the two sides. As a result, the leakage is eliminated allowing unattenuated propagation along the longitudinal direction (x). Such a condition of total reflection from the dielectric boundary between the central guide (ϵ_r) and the external substrate (ϵ'_r) is possible, only when the effective dielectric constant, ϵ_{eff}, of propagation of the dielectric-guide-coupled transmission line is greater than ϵ'_r

$$\epsilon_{\text{eff}} = \beta^2/k_0^2 > \epsilon'_r \tag{1}$$

where k_e is the propagation constant of the dielectric-guide-coupled transmission line and k_0 is the free space propagation constant. It is desirable that the width of the central dielectric guide is designed such that the dielectric-waveguide modes are not strongly coupled to. This is important in order to avoid/minimize unwanted excitation of the dielectric-waveguide mode(s) at any circuit discontinuity. It is also desirable that the relative values of ϵ_r and ϵ'_r are chosen such that the wave is highly evanescent in the external substrate region. This would be useful to avoid unwanted coupling

to an adjacent transmission line, and will require ϵ_r' to be significantly smaller than ϵ_{eff} and ϵ_r.

For wave-guidance purposes, the desirable mode of excitation for the geometry of Fig. 2 is the printed transmission line-type of mode. However, by increasing the width of the dielectric guide, a, such that the propagation constant of the dielectric-waveguide mode is close to that of the printed transmission line, a propagating dielectric-guide mode can also be strongly coupled to. Such a possibility is promising, permitting design of novel transitions between the conductor-backed transmission line and the low-loss dielectric guide, for millimeter-wave applications. This will allow convenient integration of dielectric waveguide and printed circuits.

The analyses of the two new geometries, with the shorting strips or a dielectric guide, that we will present in the following subsections share a common basis of formulation. The additional contributions due to reflections of the leakage fields from the shorting strips or the dielectric boundaries of the dielectric guide are separately derived and then added to a common solution to the central transmission line. The reflections from the shorting strips are modeled by a periodic moment method, whereas the reflections from the dielectric boundaries are obtained by matching the boundary conditions between different field components at the dielectric interfaces.

A. Analysis of a Conductor-Backed Slotline or a Coplanar Waveguide with Shorting Strips

With reference to Fig. 1, we will model the central coplanar waveguide or the slotline by replacing the electric fields, $\overline{E}_s(x, y)$, in the slot areas by equivalent magnetic currents. Equivalent magnetic currents, $+\overline{M}_s$ and $-\overline{M}_s$, are, respectively, placed just below and above the top conductor, and the slot areas are closed by continuation of the conducting plane

$$\pm\overline{M}_s(x, y) = \pm\hat{z} \times \overline{E}_s(x, y) = \pm\overline{f}(y)e^{-jk_e x}; \qquad k_e = \beta - j\alpha, \quad (2)$$

$$\overline{f}(y) = \sum_{i=1}^{N} a_i \overline{f}_i(y). \quad (3)$$

For a coplanar waveguide the x-directed basis functions are chosen with an odd symmetry, whereas the y-directed basis functions are chosen with an even symmetry, about the center line ($y = 0$).

Now, assume the total surface currents excited on the strip arrays, $\overline{h}(x, z)$, to be along the $\pm\hat{z}$ directions. Also assume that these $\pm\hat{z}$-directed currents excited on the shorting strips have an uniform variation along z as well as x. These should be good approximations for narrow strips and electrically thin parallel-plate spacings. In addition, the currents on the strip array at $y = a/2$ satisfies an even or an odd symmetry with respect to that on the strip array at $y = -a/2$, respectively for a coplanar waveguide or a slotline. With these above considerations we can write

$$\overline{h}(x, z) = \hat{z}h(x) = \hat{z}I_z \sum_{i=-\infty}^{+\infty} p(x - ib)e^{-jk_e ib}; \quad 0 \le z \le D,\ y = -a/2,$$
$$= \pm\hat{z}I_z \sum_{i=-\infty}^{+\infty} p(x - ib)e^{-jk_e ib}; \quad 0 \le z \le D,\ y = a/2, \quad (4)$$

$$\text{where, } p(x) = \begin{cases} 1/\delta, & |x| \le \delta/2; \\ 0, & \text{elsewhere.} \end{cases} \quad (5)$$

As a standard rule, used above in (4) as well as followed elsewhere in this paper, the top sign of a double-sign notation refers to a coplanar waveguide case, whereas the bottom sign refers to a slotline case.

Further assumptions are required in order that the $e^{-jk_e x}$ variation of slot fields, $\overline{E}_s(x, y)$, used in (2) is valid. The fields produced by the slotline or coplanar waveguide can be decomposed into a "bound" part tightly confined around the central guiding region, and an exponentially "growing" part propagating away from the central transmission line in transverse (y) directions [3]. Similarly, the fields produced by the strip arrays can be decomposed into a "bound" part tightly confined around the strip (at $y = \pm a/2$), and an exponentially "growing" part propagating away from the strips. We assume that the strips and the transmission lines are sufficiently far apart, such that only the propagating field components of the strips and the central transmission line directly interact with each other, whereas the bound fields do not. For most practical transmission lines, the "bound" part of the field is so tightly confined around the central transmission line, that the placement of the strips with a reasonable physical distance from the transmission line would validate the above assumption with good accuracy. Without such an assumption, the close coupling of the bound fields of the strip array (which do not have a continuous $e^{-jk_e x}$ variation along x) to the transmission line would distort the dominant propagating fields of the central transmission line. This would invalidate the assumption of an $e^{-jk_e x}$ variation of slot fields in (2).

In addition, the center-to-center separation between the strips, b, in Fig. 1 is assumed electrically small, such that only one propagating Floquet mode is produced due to the excited currents on the strip arrays. This would require

$$b \le \frac{2\pi}{k_0\sqrt{\epsilon_r} + k_e}; \quad \text{or,} \quad b \le \frac{\pi}{k_0\sqrt{\epsilon_r}} = \frac{\lambda_0}{2\sqrt{\epsilon_r}}. \quad (6)$$

In the case where the above condition is not satisfied, coupling from the strips to the central transmission line is established through more than one propagating modes with different propagation constants, even when the strips are far away from the transmission line. Under such conditions, therefore, the assumption of an $e^{-jk_e x}$ variation of the slot fields of the transmission line will not be valid.

The spectral-domain analysis of a conductor-backed transmission line, without the shorting strips, has been presented in [3]. Without the shorting strips, a Galerkin testing procedure will result in a set of N linear equations

$$\sum_{i=1}^{N} a_i Z_{ij}(k_e) = 0; \quad \text{for all } j = 1, \cdots, N. \quad (7)$$

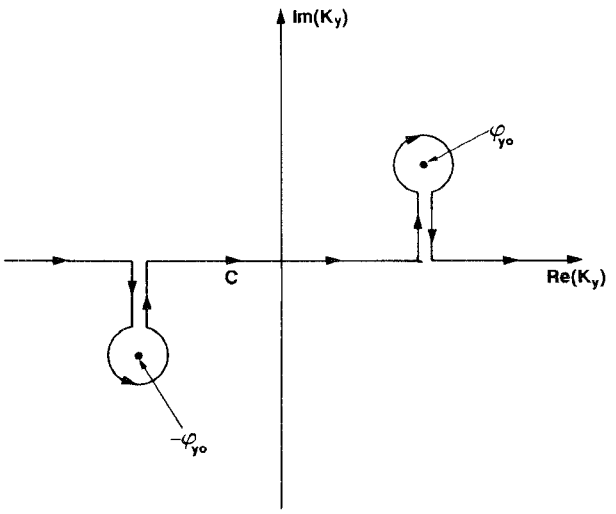

Fig. 3. The contour of integration, C, on the complex k_y plane, in order to correctly account for leakage to the parallel-plate mode

The unknown complex propagation constant, k_e, could be obtained by solving the eigenvalue matrix

$$[Z_{ij}(k_e)]_{N\times N} = 0, \tag{8}$$

$$\begin{aligned} Z_{ij}(k_e) &= \int_{slot} (\overline{H}_{i1}(y) - \overline{H}_{i2}(y)) \cdot \overline{f}_i(y) dy \\ &= \frac{1}{2\pi} \int_{-\infty,\, C}^{\infty} \overline{F}_j(-k_y) \\ &\quad \cdot [\overline{\overline{G}}_{H1M}(-k_e, k_y) + \overline{\overline{G}}_{H2M}(-k_e, k_y)] \\ &\quad \cdot \overline{F}_i(k_y) dk_y \end{aligned} \tag{9}$$

where $\overline{H}_{i1}(y)$ and $\overline{H}_{i2}(y)$ are the y-variations of the magnetic fields, respectively, below and above the groundplane at $z = D$, produced due to the ith basis mode of (3). $\overline{F}_i(k_y)$ is the Fourier transform of the ith basis function, $\overline{f}_i(y)$, and $\overline{\overline{G}}$'s are the suitable spectral-domain dyadic Green's functions [12, 11] (see Appendix for the expressions of the components of $\overline{\overline{G}}$).

It should be noted, as presented in [3], the contour of spectral integration, C, in (9) must be properly deformed around the pole due to the parallel-plate mode. The required path of integration is shown in Fig. 3. Power leaks from the transmission line in transverse directions due to coupling to this parallel-plate mode.

With inclusion of the shorting strips, the eigenvalue equations (7), (8) must be modified in order to account for the additional fields produced by the strip arrays

$$\sum_{i=1}^{N} a_i Z_{ij}(k_e) + I_z Z_{N+1,\,j}(k_e) = 0; \quad \text{for all } j = 1, \cdots, N \tag{10}$$

where the additional term, $I_z Z_{N+1,\,j}(k_e)$, is the reaction of the strip currents on the jth basis mode

$$I_z Z_{N+1,\,j}(k_e) = \int_{slot} \overline{H}_s(y) \cdot \overline{f}_j(y)\, dy. \tag{11}$$

$\overline{H}_s(y)$ is the y-variation of the magnetic field (x-variation is assumed to be $e^{-jk_e x}$) produced by the strip arrays just below the conductor at $z = D$.

Using a Floquet mode decomposition of the currents on the strip array at $y = -a/2$ (and, similarly for the strip array at $y = +a/2$ with a $\pm$ sign due to symmetry), we get

$$\overline{h}(x, z) = \hat{z} \frac{I_z}{b} \sum_{i=-\infty}^{+\infty} P\left(-k_e + \frac{2\pi i}{b}\right) e^{+j(-k_e + (2\pi i/b))x}; \quad 0 \le z \le D,\ y = -a/2 \tag{12}$$

where $P(k_x)$ is the Fourier transform of the x-variation of the strip currents, $p(x)$. Considering only the zeroth Floquet mode for coupling to the central transmission line, the magnetic field, $\overline{H}_s(x, y)$, at the transmission line produced by the two strip arrays can be expressed as

$$\begin{aligned} \overline{H}_s(x, y) &= \frac{I_z}{2b} P(-k_e) e^{-jk_e x} \left[\left(-\hat{x} + \frac{k_e}{\varphi_{y0}} \hat{y} \right) e^{-j\varphi_{y0}(y + a/2)} \right. \\ &\quad \left. \pm \left(\hat{x} + \frac{k_e}{\varphi_{y0}} \hat{y} \right) e^{j\varphi_{y0}(y - a/2)} \right] \\ &= \overline{H}_s(y) e^{-jk_e x}. \end{aligned} \tag{13}$$

$$\varphi_{yi} = \sqrt{k_0^2 \epsilon_r - \varphi_{xi}^2}; \quad \begin{aligned} &\text{Im}(\varphi_{yi}) > 0, \quad \text{Re}(\varphi_{xi}) < k_0 \sqrt{\epsilon_r}; \\ &\text{Im}(\varphi_{yi}) < 0, \quad \text{Re}(\varphi_{xi}) > k_0 \sqrt{\epsilon_r}, \end{aligned} \tag{14}$$

$$\varphi_{xi} = -k_e + \frac{2\pi}{b} i. \tag{15}$$

Using (13) in (11), and simplifying using proper symmetry of $\overline{F}_j(k_y)$ for a slotline or a coplanar waveguide, we can write

$$Z_{N+1,\,j} = \frac{e^{-j\varphi_{y0} a/2}}{b} P(-k_e) \left(-\hat{x} + \frac{k_e}{\varphi_{y0}} \hat{y} \right) \cdot \overline{F}_j(\varphi_{y0}). \tag{16}$$

An additional equation can be obtained via a Galerkin testing procedure, in order to account for the zero tangential boundary condition on the strips at $y = -a/2$. Due to the symmetry of the geometry, the tangential electric field on the strips at $y = a/2$ will be automatically satisfied

$$\sum_{i=1}^{N} a_i Z_{iN+1} + I_z Z_{N+1,\,N+1} = 0, \tag{17}$$

$$Z_{iN+1} = \int_0^D \int_{-\delta/2}^{\delta/2} E_{zi}(x, y = -a/2, z) p(x)\, dx\, dz, \tag{18}$$

$$I_z Z_{N+1,\,N+1} = \int_0^d \int_{-\delta/2}^{\delta/2} E_{zs}(x, y = -a/2, z) p(x)\, dx\, dz \tag{19}$$

where $E_{zi}(x, y, z)$ is the z-component of electric field produced due to the ith basis mode on the transmission line, and $E_{zs}(x, y, z)$ is the z-component of the electric field produced by the two strip arrays.

Using the Green's function of Appendix, $E_{zi}(x, y, z < D)$ can be expressed as

$$E_{zi}(x, y, z) = \frac{+1}{2\pi}\int_{-\infty, C, k_x=-k_e}^{\infty} \frac{j\cos(\varphi_1 z)}{\varphi_1 \sin(\varphi_1 D)} \cdot (-k_y\hat{x} - k_e\hat{y}) \cdot \overline{F}_i(k_y)e^{-jk_e x}e^{jk_y y}\, dk_y. \quad (20)$$

The contour of integration, C, is as shown in Fig. 3, of which the residue around the pole at $k_y = \varphi_{y0}$ only contributes to the propagating field far off the central transmission line for $y < 0$, whereas the residue around the other pole at $k_y = -\varphi_{y0}$ only contributes to the propagating field far off the central transmission line for $y > 0$. These propagating fields couple to the strips at $y = -a/2$ and $y = a/2$, respectively. Applying residue theorem to (20), we get

$$E_{zi}(x, y = -a/2, z) = -\frac{1}{2D\varphi_{y0}}(-\varphi_{y0}\hat{x} - k_e\hat{y}) \cdot \overline{F}_i(\varphi_{y0})e^{-jk_e x}e^{-j\varphi_{y0}a/2}. \quad (21)$$

Equation (21) can be used in (18) to get

$$Z_{iN+1} = \frac{-1}{2\varphi_{y0}}P(k_e)(-\varphi_{y0}\hat{x} - k_e\hat{y}) \cdot \overline{F}_i(\varphi_{y0})e^{-j\varphi_{y0}a/2}. \quad (22)$$

$E_{zs}(x, y, z)$ in (19) can be decomposed into a part, E_{zs1}, produced due to the strip array at $y = -a/2$, and a second part, E_{zs2}, due to the strip array at $y = a/2$, that can be derived from the Floquet mode decomposition of the source currents on the strip arrays. All Floquet modes due to the strip array at $y = -a/2$, whereas only the propagating Floquet mode due to the strip array at $y = +a/2$, contribute to the total coupling with the strip array at $y = -a/2$

$$E_{zs1}(x, y = -a/2, z) = \frac{-I_z}{b}\sum_{i=-\infty}^{+\infty}\frac{\omega\mu_0}{2\varphi_{yi}}P(\varphi_{xi})e^{j\varphi_{xi}x}; \quad 0 \le z \le D. \quad (23)$$

$$E_{zs2}(x, y = -a/2, z) = \mp\frac{\omega\mu_0}{2\varphi_{y0}}\frac{I_z}{b}P(-k_e)e^{-jk_e x}e^{-j\varphi_{y0}a}; \quad 0 \le z \le D. \quad (24)$$

Now, using (23), (24), and (19)

$$Z_{N+1,N+1} = \mp\frac{D\omega\mu_0}{2b\varphi_{y0}}P(-k_e)P(k_e)e^{-j\varphi_{y0}a} + \sum_{i=-\infty}^{+\infty}\frac{-D\omega\mu_0}{2b\varphi_{yi}}P(\varphi_{xi})P(-\varphi_{xi}) = \pm C_0 e^{-j\varphi_{y0}a} + \sum_{i=-\infty}^{+\infty} C_i \quad (25)$$

The $(N+1)$-set of eigen equations (10), (17) can be solved for the propagation constant, k_e, with the expressions for Z_{ij}'s, $i = 1, \cdots, N+1$, $j = 1, \cdots, N+1$, obtained from (9), (16), (22), (25). The complex propagation constant, k_e, is the root of the eigen-matrix equation

$$[Z_{ij}(k_e)]_{(N+1)\times(N+1)} = 0 \quad (26)$$

that can be searched using a Newton–Raphson algorithm.

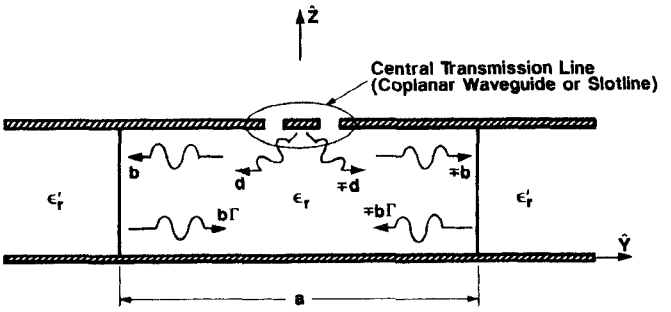

Fig. 4. Propagating x-component of magnetic field, H_x, at the dielectric interfaces at $y = +a/2$ and $y = -a/2$, far away from the central transmission line. The $-$ or $+$ sign is chosen for a coplanar waveguide or a slotline geometry, respectively, due to appropriate symmetry considerations.

B. Analysis of Conductor-Backed Slotline or Coplanar Waveguide Coupled to a Dielectric Guide

We assume that the dielectric interfaces at $y = a/2$ and $y = -a/2$ (see Fig. 2) to be sufficiently far away from the central transmission line. This is a valid assumption for most practical cases, where a reasonable width of the dielectric guide, a, will be usually larger than the extent of the tightly confined fields of the central transmission line. Under such assumption, only the propagation field components excited from the central transmission line couple to the dielectric interfaces. The propagating x-component of the magnetic field, H_x, can be written as (see Fig. 4)

$$\begin{aligned} H_x(x, y, z) &= be^{-jk_e x}(e^{+j\varphi_{yp}(y+a/2)} + \Gamma e^{-j\varphi_{yp}(y+a/2)}); \\ &\quad -a/2 < y < 0, \\ &= \mp be^{-jk_e x}(e^{-j\varphi_{yp}(y-a/2)} + \Gamma e^{+j\varphi_{yp}(y-a/2)}); \\ &\quad 0 < y < a/2, \\ &= \mp be^{jk_e x}(1+\Gamma)e^{-j\varphi'_{yp}(y-a/2)}; \quad y > a/2, \\ &= be^{-jk_e x}(1+\Gamma)e^{j\varphi'_{yp}(y+a/2)}; \quad y < -a/2. \end{aligned} \quad (27)$$

$$\varphi_{yp} = \sqrt{k_0^2\epsilon_r - k_e^2}; \quad \mathrm{Im}(\varphi_{yp}) > 0, \quad (28)$$

$$\varphi'_{yp} = \sqrt{k_0^2\epsilon'_r - k_e^2}; \quad \begin{aligned} &\mathrm{Im}(\varphi'_{yp}) < 0, \beta > k_0\sqrt{\epsilon'_r}; \\ &\mathrm{Im}(\varphi'_{yp}) > 0, \beta < k_0\sqrt{\epsilon'_r}, \end{aligned} \quad (29)$$

$$\Gamma = \frac{-\varphi_{yp} + \varphi'_{yp}}{\varphi_{yp} + \varphi'_{yp}} \quad (30)$$

where Γ is the reflection coefficient of H_x at the dielectric interfaces, and φ_{yp} is the same as φ_{y0} in (14), equal to the pole due to the parallel-plate mode in the complex k_y plane.

Without the dielectric interface, the conductor backed slotline or coplanar waveguide with a uniform dielectric, ϵ_r, between the parallel plates, can be analyzed using a method presented in [3]. This results in the eigenvalue equations (7), (8), that can be solved for the complex propagation constant, k_e. With the inclusion of the dielectric interfaces at $y = \pm a/2$, the above eigenvalue equations (7), (8) must be modified in order to include the additional reflections from the interfaces

$$\sum_{i=1}^{N} a_i Z_{ij}(k_e) + bZ_{N+1,j}(k_e) = 0; \quad \text{for all } j = 1, \cdots, N \tag{31}$$

where the new term, $bZ_{N+1,j}(k_e)$, is the reaction of the magnetic fields, $\overline{H}_r(x, y, z)$, reflected from the dielectric interfaces at $y = \pm a/2$, on the jth basis mode of the transmission line

$$bZ_{N+1,j}(k_e) = \int_{slot} \overline{H}_r(y) \cdot \overline{f}_j(y)\, dy. \tag{32}$$

$\overline{H}_r(y)$ is the y-variation of $\overline{H}_r(x, y, z)$ just below the top conductor at $z = D$. From the reflected parts of H_x in (27), and using simple field relationships in a parallel plate structure, the reflected magnetic field, $\overline{H}_r(x, y, z)$, can be expressed as

$$\begin{aligned}\overline{H}_r(x, y, z) &= b\Gamma e^{-jk_e x}\left[\left(\hat{x} - \frac{k_e}{\varphi_{yp}}\hat{y}\right)e^{-j\varphi_{yp}(y+a/2)}\right. \\ &\quad \left. \mp \left(\hat{x} + \frac{k_e}{\varphi_{yp}}\hat{y}\right)e^{+j\varphi_{yp}(y-a/2)}\right] \\ &= \overline{H}_r(y)e^{jk_e x}; \quad -a/2 < y < a/2. \end{aligned} \tag{33}$$

Using (33) in (32), and simplifying using the symmetry conditions for the basis transforms, $\overline{F}_j(k_y)$, we get

$$Z_{N+1,j} = 2\Gamma e^{-j\varphi_{yp}a/2}\left[\left(\hat{x} - \frac{k_e}{\varphi_{yp}}\hat{y}\right) \cdot \overline{F}_j(\varphi_{yp})\right]. \tag{34}$$

An additional linear equation involving the N-unknown basis coefficients, a_i's, and the unknown coefficient, b, can be obtained. If the propagating part of H_x excited by the transmission line in the $y < 0$ direction is $de^{+j\varphi_{yp}y}e^{-jk_e x}$, then with reference to the Fig. 4

$$b = de^{-j\varphi_{yp}a/2} \mp b\Gamma e^{-j\varphi_{yp}a} \tag{35}$$

which can be simplified as

$$\left(\frac{e^{-j\varphi_{yp}a/2}}{1 \pm \Gamma e^{-j\varphi_{yp}a}}\right)d - b = \left(\frac{e^{-j\varphi_{yp}a/2}}{1 \pm \Gamma e^{-j\varphi_{yp}a}}\right)\left(\sum_{i=1}^{N} d_i\right) - b = 0, \tag{36}$$

$$\sum_{i=1}^{N} a_i Z_{iN+1} - b = 0, \tag{37}$$

$$Z_{iN+1} = \frac{d_i}{a_i}\left(\frac{e^{-j\varphi_{yp}a/2}}{1 \pm \Gamma e^{-j\varphi_{yp}a}}\right) \tag{38}$$

where d_i is coefficient of the propagating part of H_x, excited in $y < 0$ direction by the ith basis mode, $\overline{M}_s = \pm a_i \overline{f}_i(y)e^{-jk_e x}$ (see (2)).

Using the spectral Green's functions of Appendix, the x-component of magnetic field, $H_{xi}(x, y, z)$, excited by the ith basis mode, $\overline{f}_i(y)$, can be expressed as

$$\begin{aligned} H_{xi}(x, y, z) &= \frac{+1}{2\pi}\int_{-\infty, C}^{\infty} \hat{x} \cdot \bar{\bar{G}}_{H1M}(-k_e, k_y, z) \\ &\quad \cdot \overline{F}_i(k_y)a_i e^{jk_e x}e^{jk_y y}\, dk_y \\ &= \frac{+1}{2\pi}\int_{C, k_x = -k_e} \frac{\cos(\varphi_1 z)}{\varphi_1 \omega\mu_0 \sin(\varphi_1 D)} \\ &\quad \cdot (jk_e k_y \hat{y} + j(k_0^2\epsilon_r - k_e^2)\hat{x}) \\ &\quad \cdot \overline{F}_i(k_y)a_i e^{-jk_e x}e^{jk_y y}\, dk_y \end{aligned} \tag{39}$$

where the contour of integration, C, is as defined in Fig. 3. The residue part of integration around the pole at φ_{yp} (φ_{y0} in Fig. 3) only contribute to the propagating component of H_x for $y < 0$. Using residue theory

$$\begin{aligned} d_i e^{-jk_e x}e^{+j\varphi_{yp}y} &= -e^{-jk_e x}e^{+j\varphi_{yp}y} \\ &\quad \left[\frac{a_i \overline{F}_i(\varphi_{yp})}{2\omega\mu_0 D} \cdot (\varphi_{yp}\hat{x} + k_e\hat{y})\right] \end{aligned} \tag{40}$$

Using (40) in (38), we get

$$Z_{iN+1} = \frac{-\overline{F}_i(\varphi_{yp})}{2\omega\mu_0 D} \cdot (\varphi_{yp}\hat{x} + k_e\hat{y})\left(\frac{e^{-j\varphi_{yp}a/2}}{1 \pm \Gamma e^{-j\varphi_{yp}a}}\right). \tag{41}$$

Now, the $(N + 1)$ set of eigen equations (31), (37) can be solved for the propagation constant, k_e, with the expressions for Z_{ij}'s, $i = 1, \cdots, N + 1$; $j = 1, \cdots, N + 1$, obtained from (9), (34), and (41). k_e is the root of the eigen-matrix equation

$$[Z_{ij}(k_e)]_{(N+1)\times(N+1)} = 0. \tag{42}$$

III. Results

A. Leakage Suppression Using Shorting Strips/Pins

Using a minimal number of shorting pins, optimally placed around a transmission line circuit, is a feasible approach for leakage suppression in MMIC's, hybrid circuits, as well as interconnect packages. Our analysis evaluates the effects of the positioning parameters on the leakage suppression level. Figs. 5 and 6 show the results of leakage suppression in a conductor-backed coplanar waveguide, as a function of the width, δ, of the shorting strips, center-to-center separation, b, between the strips, and the distance, $a/2$, between the strips and the center of the transmission line. Clearly, the power leakage has been significantly suppressed. As Fig. 5 shows, in order to reduce the attenuation, α, it is desirable to place the shorting strips as close to the center of the coplanar waveguide as possible. however, the shorting strips should not be too close to the slot edges, which may result in undesirable interference with the central bound fields of the transmission line.

A sharp increase in attenuation can be observed in Fig. 5 when the distance, a, between the shorting strips and the center of the transmission line approaches a critical value a_c

$$a_c = \frac{\pi}{Re(\varphi_{y0})} \simeq \frac{\pi}{\sqrt{k_0^2\epsilon_r - \beta^2}}; \; \beta < k_0\sqrt{\epsilon_r} \tag{43}$$

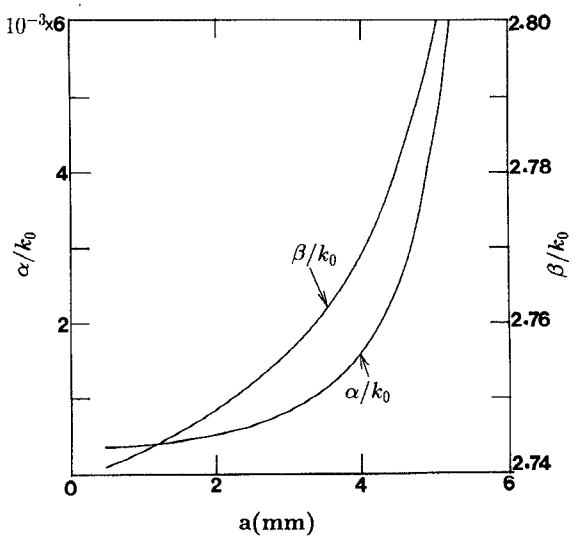

Fig. 5. Propagation, β, and attenuation, α, constants normalized to free-space wave number, k_0, of a conductor-backed coplanar waveguide geometry (see Fig. 1) as a function of the separation, a, between the two symmetric rows of strips. $W = 0.1$ mm, $S = 0.2$ mm, frequency = 10 GHz, $\epsilon_r = 13$, $D = 0.2$ mm, $\delta = 0.1$ mm, $b = 1$ mm. Notice the leakage increases as a approaches $a_c \simeq 6.5$ mm. The results beyond $a = 5$ mm, with much higher α are not shown.

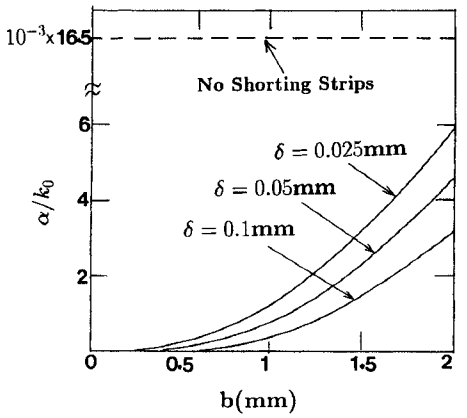

Fig. 6. Attenuation constant, α, normalized to the free space wave number, k_0, of the conductor-backed coplanar waveguide geometry of Fig. 5 with $a = 1$ mm, as a function of center-to-center separation, b, between shorting strips, for different values of strip widths, δ.

where φ_{y0} is given by (14), and β is obtained from Fig. 5. It may be noted that the leakage level close to $a = a_c$ is significantly large compared to that for smaller values of a, making the use of the shorting pins/strips ineffective in this region. The leakage loss close to $a = a_c$ can increase to levels comparable to, sometimes significantly larger than that without any shorting pins. Besides, close to and beyond $a = a_c$, complex mode-coupling with the rectangular waveguide-like modes (confined between the top and bottom conductors of the parallel-plate structure, and the two conductor-like strip walls at $y = \pm a/2$) would occur, making it undesirable to use such larger a for practical designs.

The resonance effect in Fig. 5 close to $a = a_c$, showing sharp increase in the attenuation, α, can be explained by interference of the direct leakage fields excited by the central transmission line with the multiple reflections from the shorting strips. For the transverse propagation of the parallel-plate wave, the value of $a = a_c$ corresponds to a quarter wavelength between the shorting strips and the center of the transmission line (see Fig. 1). Hence, the leakage field that is transversally excited by the coplanar waveguide to one side (say, in $+\hat{y}$ direction), partly (significantly) reflects back from the shorting strips at $y = a/2$ with about the same phase. Further, as can be seen from the field symmetry, the parallel-plate leakage fields excited from the coplanar waveguide directly in the $-\hat{y}$ direction is in phase with that in the $+\hat{y}$ direction. (Note, in contrast, for a conductor-backed slotline these leakage fields excited to the two sides are 180 degrees out of phase with each other.) Therefore, the above in-phase reflected field from the strips at $y = a/2$ will constructively interfere with the direct leakage field excited in the $-\hat{y}$ direction. Together they partly escape through the strips at $y = -a/2$, and the rest reflects back in the $+\hat{y}$ direction, which in turn experiences multiple reflections and transmissions through the strip arrays. The round-trip multiple reflections from the strip arrays also constructively interfere with each other when a approaches a_c. Accordingly, the constructive interference together of all the direct as well as the multiply reflected leakage fields result in the increased loss in Fig. 5, as a approaches a_c.

Fig. 6 shows the variation of leakage with strip width, δ, and the center-to-center separation, b. As expected, leakage loss increases as the center-to-center separation between shorting strips is increased, because it leaves more open area between the strips for the leakage power to escape through. Also due to the same reason, the leakage loss is seen to increase for reduced strip widths. It maybe reminded, however, that the center-to-center separation between the shorting strips, b, should not be larger than a limiting value given by (6), in order to avoid moding problems due to the excitation of higher order Floquet modes from the strip arrays.

Figs. 7 and 8 show the results of leakage suppression in conductor-backed slotlines, that can be compared and contrasted with the corresponding results from Figs. 5 and 6 for a conductor-backed coplanar waveguide. The dependence of leakage in Fig. 8 on strip width, δ, and center-to-center separation between the shorting strips, b, show similar trends as in Fig. 6. However, the results of leakage loss, α, in Fig. 7 for a conductor-backed slotline can be seen in distinct contrast with the results of Fig. 5 for a conductor-backed coplanar waveguide. Unlike in Fig. 5, in Fig. 7 α decreases as the shorting strips are placed farther away from the center of the slotline and goes to a minimum at the critical value of $a = a_c$, given approximately by (43). With the similar arguments made earlier for a conductor-backed coplanar waveguide, the minimum value of α for the conductor-backed slotline at $a \simeq a_c$ can be explained due to a destructive interference of the leakage fields. This is because the two leakage fields excited by the conductor-backed slotline to the two sides are now out of phase with each other, unlike being in phase for a conductor-backed coplanar waveguide.

To comprehend, the placement of the shorting strips/pins critically determine the level of leakage suppression that can be achieved. For a conductor-backed coplanar waveguide

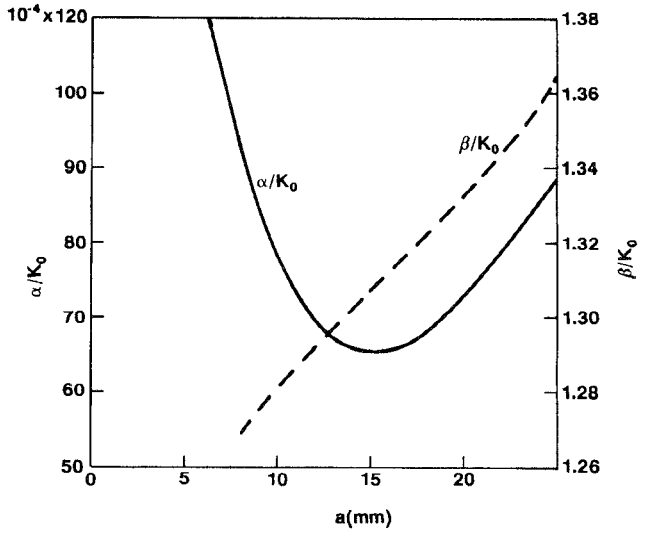

Fig. 7. Propagation, β, and attenuation, α, constants normalized to free-space wave number, k_0, of a conductor-backed slotline geometry (see Fig. 1) as a function of the separation, a, between the two symmetric rows of strips. $W = 1$ mm, frequency $= 10$ GHz, $\epsilon_r = 2.55$, $D = 8.01$ mm, $\delta = 1$ mm, $b = 7$ mm. Notice the minimum leakage at $a = a_c \simeq 15$ mm. The value of α for the geometry without the shorting strips is about $0.1\ k_0$.

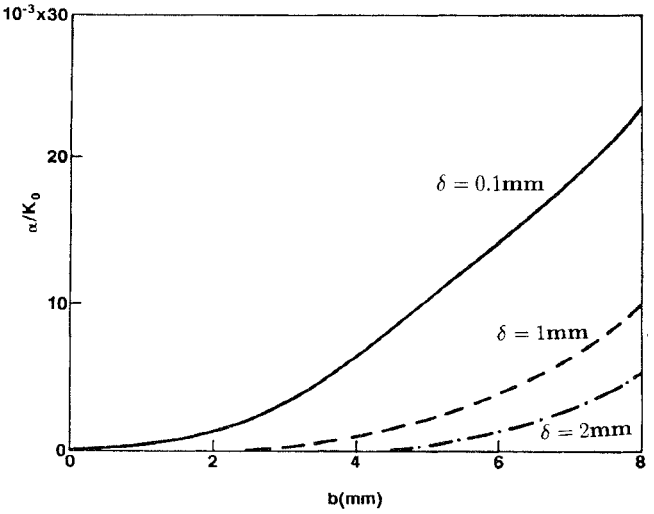

Fig. 8. Attenuation constant, α, normalized to the free-space wave number, k_0, of the conductor-backed slotline geometry of Fig 7 with $a = 15$ mm, as a function of center-to-center separation, b, between shorting strips, for different values of strip widths, δ.

the shorting pins should be placed as close to the central transmission line as possible, without interfering with the central bound fields of the transmission line. Typically, the bound fields of the coplanar waveguide transversely extend over a distance of the order of one slot width beyond the side edges. Therefore, for best results, the shorting pins should be placed about one slot-width distance away from the transverse edges. For a conductor-backed slotline, on the other hand, the shorting pins should be placed at a distance $a/2 = a_c/2$, as given by (43), for optimum performance. Besides, the distance between the consecutive pins along the longitudinal (x) direction should be less than $\lambda_0/(2\sqrt{\epsilon_r})$ in order to avoid multiple moding problems, as discussed before. Computations similar to Figs. 8 and 6 should be used to determine the required spacing, b, that provides an acceptable leakage level.

B. Leakage Avoidance Using Dielectric-Guide-Coupled Geometries

By fabricating a small dielectric groove under a conductor-backed slotline or coplanar waveguide, one can avoid the parallel-plate leakage problem. As discussed, such transmission line geometries would be attractive for mixed integration of printed circuits with dielectric-guide devices. Figs. 9 and 10 show the results of leakage constant, α, in a conductor-backed coplanar waveguide and a slotline, respectively, coupled to a dielectric guide. Consistent with the condition (1), in both cases the attenuation, α, is zero when $\epsilon_r' < (\beta/k_0)^2$ (see Fig. 2). It is seen from computation, that the phase constant, β, in both example cases is not strongly affected by the outer dielectric constant, ϵ_r', or the width, a, of the dielectric guide (except in the regions of strong coupling to the dielectric-waveguide mode). Therefore, as per (1), in Figs. 9 and 10 the threshold value of ϵ_r' between the leaky and the nonleaky regions is practically independent of ϵ_r' and a. It is interesting to see that the leakage attenuation can also be reduced to an arbitrary low value by having the dielectric constant of the outer medium significantly higher than that of the central dielectric guide region. Further, as expected, in both cases of Figs. 9 and 10 the values of α are the same for all values of a, when $\epsilon_r' = \epsilon_r$, because the geometry now turns into a regular conductor-backed geometry with a uniform dielectric medium between the parallel plates. When $\epsilon_r > \epsilon_r' > (\beta/k_0)^2$ the conductor-backed coplanar waveguide in Fig. 9 exhibits less leakage for wider guides (larger a), but when $\epsilon_r' > \epsilon_r$ it exhibits more leakage for wider guides. The above trends are seen to have reversed for a conductor-backed slotline in Fig. 10. As in conductor-backed geometries with shorting strips, such trends of α for different values of a can be explained by interference of the reflected leakage fields from the dielectric boundaries at $y = \pm a/2$ (see Fig. 2).

Notice in Figs. 9 and 10 that at the onset of leakage when ϵ_r' is slightly greater than $(\beta/k_0)^2$, there is a sharp increase of α for the conductor-backed slotline as well as the conductor-backed coplanar waveguide. At this value of ϵ_r' the transverse propagation constant in outer dielectric is zero, resulting in a unity reflection coefficient for the parallel-plate mode. Therefore, the dielectric interface at this critical value of ϵ_r' acts like a perfect open circuit, which is a dual condition to the short-circuiting effects of the shorting strips discussed in the last section. Using dual arguments to that in last Section III-A, one can explain the relative trends of α in Figs. 9 and Fig. 10 with "a," at the onset of leakage ($\epsilon_r' = (\beta/k_0)^2$). Accordingly, these trends can be seen in contrast to the respective trends of Figs. 5 and 7, with shorting strips. For a conductor-backed coplanar waveguide, the leakage loss in Fig. 9 at the critical value of ϵ_r' reduces with increasing a, whereas in Fig. 5 the leakage loss with shorting strips increases with increasing a. Similarly, for a conductor-backed slotline, the leakage loss in Fig. 10 at the critical value of ϵ_r' increases with increasing a, whereas for the corresponding range of a the leakage loss in Fig. 7 with shorting strips reduces with increasing a.

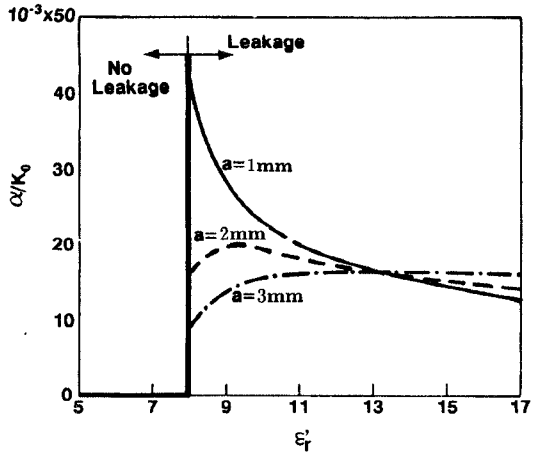

Fig. 9. Attenuation constant, α, normalized to the free space wave number, k_0, of a modified conductor-backed coplanar waveguide of Fig. 2 with $\epsilon_r = 13$, $D = 0.2$ mm, $W = 0.1$ mm, $S = 0.2$ mm, frequency = 10 GHz, for different values of a, as a function of the external dielectric constant, ϵ_r'. Propagation constant, β, does not change significantly; $2.73 < \beta/k_0 < 2.78$. Note that the threshold value of ϵ_r' between power leakage and no leakage is strictly a function of a, but here is approximately the same ($\epsilon_r' \simeq 8$) for the three values of a.

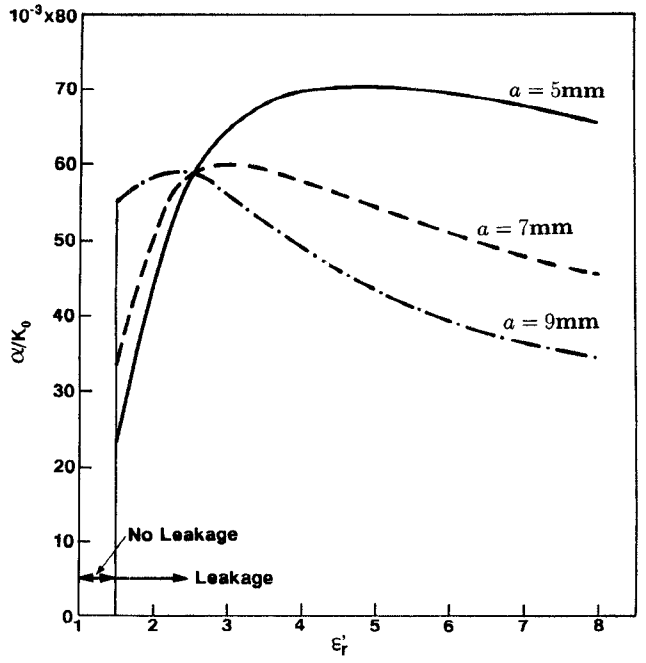

Fig. 10. Attenuation constant, α, normalized to the free-space wave number, k_0 of a modified conductor-backed slotline of Fig. 2 with $\epsilon_r = 2.55$, $D = 8.01$ mm, $W = 1$ mm, frequency = 10 GHz, for different values of a, as a function of ϵ_r'. The threshold value of $\epsilon_r' \simeq 1.5$ between leakage and no leakage conditions is only approximately the same for the three values of a.

As we discussed, the leakage is eliminated when the outer dielectric, ϵ_r', is smaller than $(\beta/k_0)^2$. In this no-leakage region of ϵ_r', the design of the width, a, of the dielectric guide can also be critical. Figs. 11 and 12 show the propagation characteristics of the dielectric-guide-coupled geometries of Figs. 9 and 10, respectively. As can be clearly seen, normally the propagation constant, β is not a strong function of the guide width, a. However, when the width is changed such that the propagation constant of an appropriate dielectric-

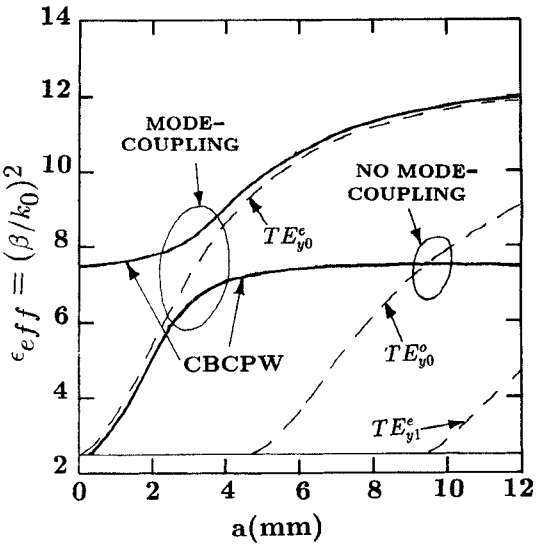

Fig. 11. Propagation characteristics of the modified conductor-backed coplanar waveguide of Fig. 9, with $\epsilon_r' = 2.5$, as a function of the guide width, a. Propagation characteristics of the different dielectric-waveguide modes are also shown indicating coupling to appropriate cases.

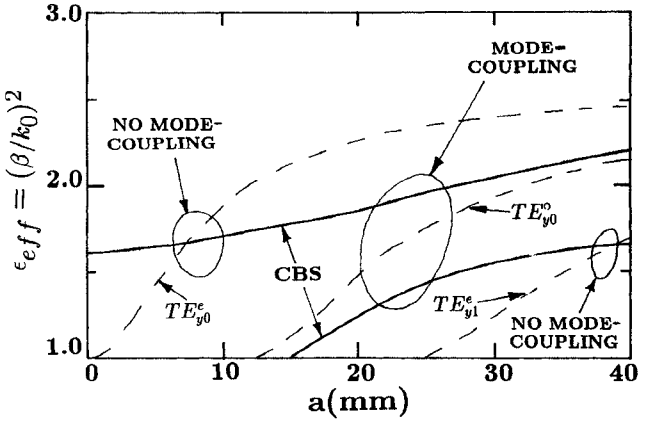

Fig. 12. Propagation characteristics of the modified conductor-backed coplanar waveguide of Fig. 10, with $\epsilon_r' = 1.0$, as a function of the guide width, a. propagation characteristics of the different dielectric-waveguide modes are also shown indicating coupling to appropriate cases.

waveguide mode is close to β, the dielectric-waveguide and the dominant printed transmission line-type modes strongly interact with each other. This results in the "mode-splitting" effects of Figs. 11 and 12 in the vicinity of the coupling regions. It should be noted that the parallel-plate mode excited from the central transmission line only couples to the TE_y dielectric modes. Further, due to the field symmetries, the coplanar waveguide geometry of Fig. 11 couples only to the TE_y^e dielectric modes with an even distribution of the electric field with respect to y, whereas the slotline geometry of Fig. 12 couples only to the TE_y^o dielectric modes with an odd distribution of the electric fields with respect to y. For waveguidance purposes, when coupling to the dielectric-modes is not desirable, the width a must be designed far off the strong "mode-coupling" regions. For the example case of Figs. 11 and 12, the value of a can be safely designed up to about 0.1 cm and 1.0 cm, respectively. However, with proper

selection of the width a in the vicinity of the "mode-coupling" regions, strong coupling to the dielectric-waveguide modes can be deliberately established allowing the design of novel transition devices between the printed transmission line and the dielectric-waveguide.

C. Leakage Avoidance in Conductor-Backed Geometries Using Two Substrate Layers Between Parallel Plates

The many attractive advantages of using a conductor backing under the substrate of a slotline or a coplanar waveguide can still be availed, while eliminating the undesired power leakage to the parallel-plate mode, by placing the conductor backing slightly below the primary substrate. A second substrate of a lower dielectric constant may be inserted as a spacer between the primary substrate and the conductor backing. The insertion of the low dielectric constant substrate reduces the propagation constant of the parallel-plate mode, while only minimally affecting the printed transmission line mode. With a proper choice of the dielectric constant, ϵ_{r2}, and thickness, h, of the spacer substrate, the effective dielectric constant of the parallel-plate mode, $\epsilon_{\text{eff}}(PP)$, can be sufficiently reduced below that of the slotline or the coplanar waveguide, ϵ_{eff}. As a result, the no-leakage condition of propagation [3] is satisfied. Of related interest is the work of [14], where a two-layer conductor-backing configuration was proposed for reducing mode conversion at discontinuities in conductor-backed coplanar waveguides.

Fig. 13(a) and (b) show the variation of ϵ_{eff} and $\epsilon_{\text{eff}}(PP)$ with the spacing height, h, for a conductor-backed slotline and coplanar waveguide, respectively. The threshold values of h for the onset of leakage can be seen when the ϵ_{eff} graphs of the transmission lines intersect the corresponding $\epsilon_{\text{eff}}(PP)$ curves. As expected, a smaller threshold value of h is seen for a lower value of ϵ_{r2}. Further, the ϵ_{eff} for a coplanar waveguide is considerably higher than that of a slotline with the same substrate and slot width. Therefore, a considerably smaller threshold value of the spacer height, h, is required in order to bring down the $\epsilon_{\text{eff}}(PP)$ below the ϵ_{eff} of a coplanar waveguide, as compared to that of a slotline. This can be seen from Fig 13(a) and (b). In either case of a conductor-backed slotline or a coplanar waveguide, it is seen that only a moderately thick spacer is necessary to eliminate the power leakage.

In Fig. 13(a) and (b) the ϵ_{eff} curves for the transmission line modes are shown to directly extend from the nonleaky into the leakage regions. This is only a simplistic picture of immediate transition from a leaky to a nonleaky behavior. Actually, in the intersecting regions between the ϵ_{eff} and $\epsilon_{\text{eff(PP)}}$ curves in Fig. 13, a complex mode-transition phenomenon occurs [7], that has also been discussed in [13] for practical finite-length circuits. Instead of a single mode, there actually exist two modes, one leaky and the other nonleaky (sometimes with other modal behavior [7]). As the operating point approaches the transition region, a mixture of more than one mode, with gradually varying individual contributions, is excited by any practical circuit. Therefore, instead of an immediate transition from a purely leaky to a purely nonleaky mode of

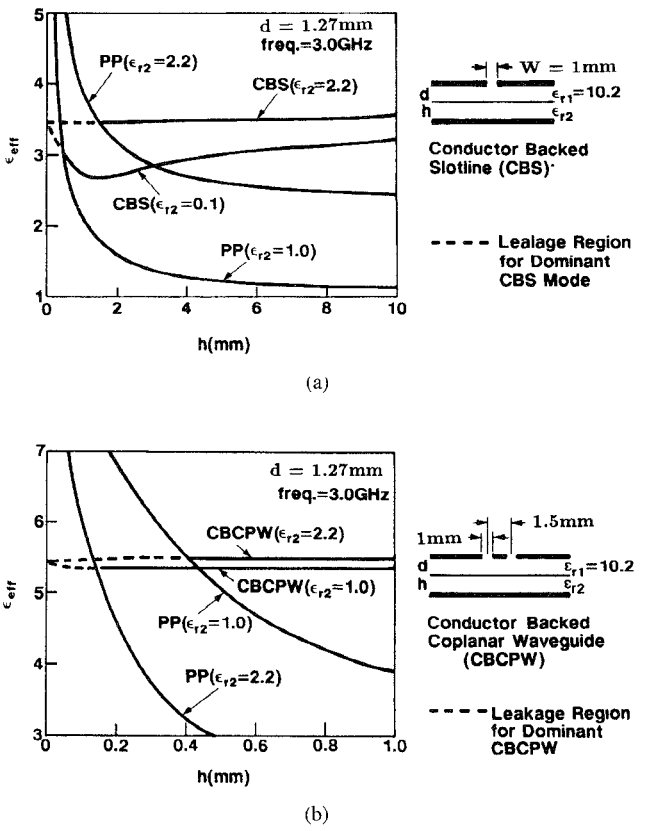

Fig. 13. Effective dielectric constant, ϵ_{eff}, of the parallel-plate mode (PP), as compared with the effective dielectric constant, of (a) the conductor-backed slotline (CBS) mode, (b) the conductor-backed coplanar waveguide mode (CBCPW), as a function of h, showing the avoidance of leakage for suitable design of h and ϵ_{r2}. Two sets of data for $\epsilon_{r2} = 1.0$ (air), and $\epsilon_{r2} = 2.2$ are presented.

propagation as shown in Fig. 13, for practical circuits there exist finite regions around the transition points in Fig. 13 over which there is a gradual transition from a leaky into a nonleaky mode of propagation. Accordingly, even when ϵ_{eff} of the transmission line in Fig. 13 is larger than (close to, but sometimes appreciably larger than $\epsilon_{\text{eff}}(PP)$) a practical finite-length section of the transmission line could still suffer from appreciable power leakage due to significant excitation of a leaky parallel-plate type mode, [13]. It is important to identify such unsafe regions around the transition points in Fig. 13, that should be avoided in practical designs.

To demonstrate this unsafe region, we have made a rigorous 3-D moment method analysis [13] of a realistic circuit. The circuit consists of two parallel shorted stubs of a conductor-backed slotline of Fig. 13(a), excited at the center by a delta-gap current source. The results of the voltage distribution along the slotline section are plotted in Fig. 14, from which the attenuation behavior can be qualitatively estimated. As can be seen from Fig. 14, when the spacer is not used ($h = 0$) the slotline is significantly leaky, but the leakage has been clearly suppressed by use of the spacer, as expected from the results of Fig. 13. From Fig. 13(a), notice that the threshold value of h for the same slotline parameters ($\epsilon_{r2} = 2.2$) is about 1.5 mm. However, as Fig. 14 confirms, there is significant power leakage when $h = 2$ mm, though it is in the nonleaky region

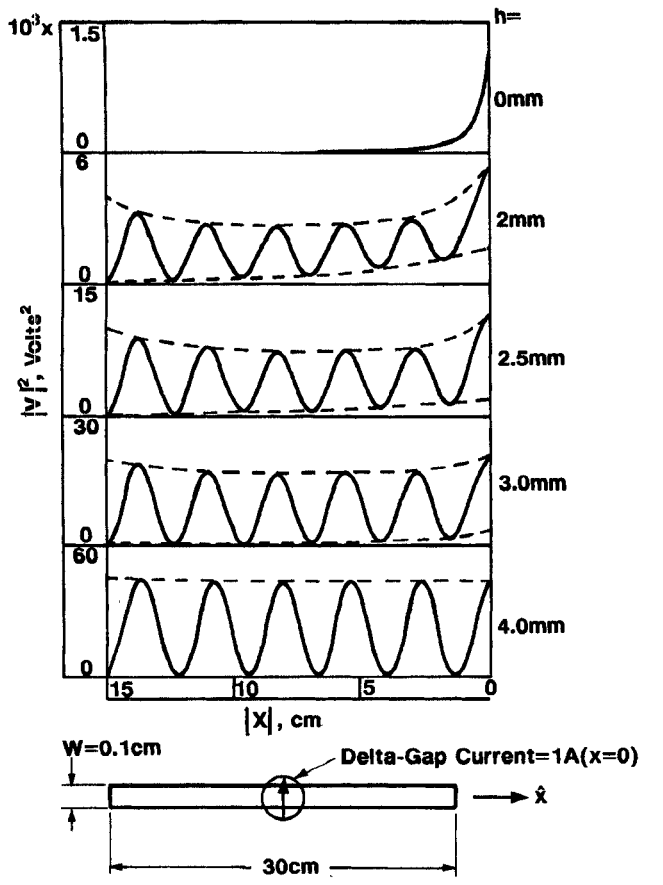

Fig. 14. Distribution of the slot voltages along a slotline stub geometry. The slotline is conductor-backed with $w = 1$ mm, $\epsilon_{r1} = 10.2$, $d = 1.27$ mm, using a spacer of $\epsilon_{r2} = 2.2$, and spacer thickness, h (see Fig. 13(a) for the geometry of the conductor-backing geometry). Frequency of operation = 10 GHz, and the length of the slotline section = 30 cm, excited at the center by a delta-gap current source of $1A$.

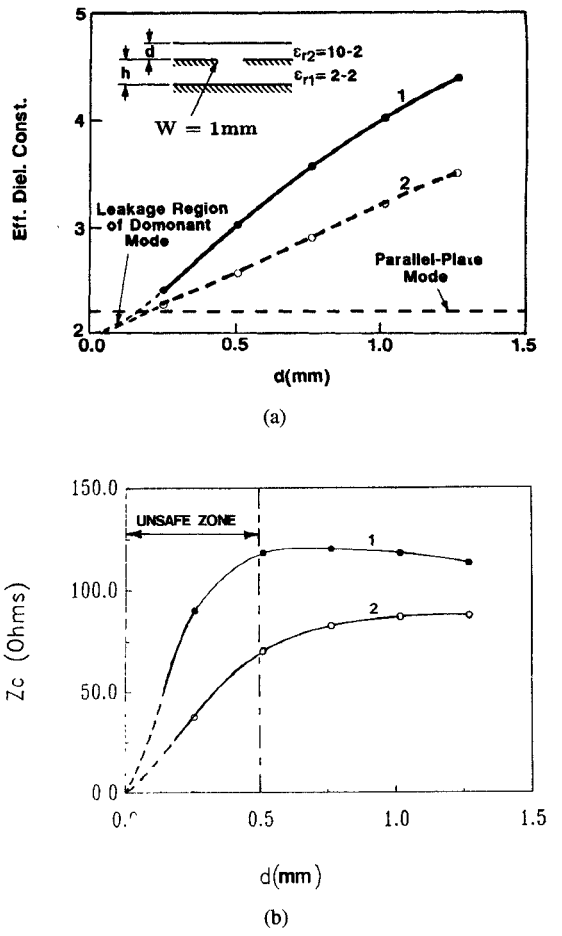

Fig. 15. (a) Effective dielectric constants, and (b) characteristic impedance, of a loaded conductor-backed slotline with the cover dielectric constant, $\epsilon_{r2} = 10.2$, parallel-plate dielectric constant, $\epsilon_{r1} = 2.2$, as a function of cover thickness d, at frequency = 10 GHz; Curve 1) $h = 1.57$ mm; Curve 2) $h = 0.76$ mm.

of Fig. 13(a). Appreciable leakage can be seen in Fig. 14 even up to $h = 3$ mm. Accordingly, the spacing height, h, should be designed greater than about 3 mm, not just greater than 1.5 mm as predicted from Fig. 13. Depending on the individual physical parameters, the transition region may extend much farther above the transition point. Similar analyses can be used to determine the unsafe zones of operation in individual leakage situations.

D. Leakage Avoidance in Conductor-Backed Geometries Using Dielectric Loading

When other practical considerations allow, the leakage in conductor-backed geometries can also be avoided by placing a thin substrate of high dielectric constant on top of the transmission line. This concept was first introduced by us for a conductor-backed slotline in [15], that has recently been used also to coplanar waveguides in [16]. In principle, the idea is similar to the leakage suppression method discussed in the last section. The dielectric loading on top will increase the effective dielectric constant, $\epsilon_{\text{eff}} = (k_e/k_0)^2$, of the transmission line above that of the parallel-plate mode, while keeping the parallel-plate mode unaffected. As a result, the no leakage condition of propagation [3] would be satisfied for a proper design of the cover layer. This method of avoidance of leakage is demonstrated from our computed results of Fig. 15. Fig. 15 shows the variation of ϵ_{eff} and the corresponding characteristic impedance, Z_c, for a conductor-backed slotline, as a function of the cover thickness, d. Data for two values of the parallel-plate thickness, h, have been presented. As can be seen, for d larger than a threshold value (about 0.12 mm) the effective dielectric constant, ϵ_{eff}, is larger than the uniform dielectric constant between the parallel plates, ϵ_{r1}. In this range, therefore, the above condition of no leakage [3] is satisfied, allowing unattenuated propagation along the transmission line.

As a matter of caution, a cover height, d, sufficiently larger than the threshold value should always be used in order to ensure no leakage in practical designs. For values of d greater than but closer to (sometimes significantly larger than) the threshold value, the unwanted leakage may still be significantly excited in practical finite-length circuits. This is similar to the situation discussed in the last section. As demonstrated in the last section, such unsafe region of operation can be determined using a rigorous 3-D analysis of a practical finite-length circuit.

Characteristic impedances, Z_c, in the nonleaky regions of Fig. 15(a) are computed using a power-voltage definition, and

the results are presented in Fig. 15(b) (extrapolated into the transition region). As can be seen in Fig. 15(b), Z_c values sharply decrease when the ϵ_{eff} curves approach the leakage zone ($\epsilon_{\text{eff}} \simeq \epsilon_{r1}$). Such sharp decrease of Z_c close of a leakage transition region is a usual behavior also seen in other transmission lines. This is because, the transverse fields of the transmission line start to spread away from the central region, as the operating point gets close to the transition zone. This field spreading is equivalent to an increase of the transverse power of the nonleaky mode for a given slot voltage, and, therefore, a sharp reduction in the values of Z_c computed by a power-voltage definition.

Interestingly, in the region when the transverse fields of the primary nonleaky mode start to exhibit a spreading behavior away from the center of the transmission line, or equivalently when the characteristic impedance significantly drops as explained, the spreading part of the fields has close similarity with the background parallel-plate mode. Therefore, in this region the parallel-plate leakage mode tends to get more excited by (or coupled to) the primary nonleaky mode of the transmission line. Accordingly, this region of sharp change in Z_c is a clear indication of onset of the leakage excitation, and should be avoided in practical designs. For the geometry of Fig. 15(b), this unsafe zone can be seen to extend up till about $d = 0.5$ mm. This conclusion is also in confirmation with separate rigorous simulations similar to Fig. 14 we have performed for realistic finite-length circuits.

IV. Circuits

Our investigation has demonstrated that the unwanted leakage in conductor-backed transmission lines can be eliminated, or significantly suppressed, using the proposed techniques. Such methods should find useful applications in integrated circuits and phase arrays, allowing novel use of the conductor-backed geometries. Useful design guidelines have been given for practical implementation of the suppression methods.

Appendix

A. Expressions for Green's Function Components Used in Section II

$$\hat{x}\cdot\bar{\bar{\tilde{G}}}_{H2M}\cdot\hat{x}=\tilde{G}_{H_x2M_x}(k_x,k_y)=-\frac{(k_0^2-k_x^2)}{\varphi_2\omega\mu_0}e^{-j\varphi_2(z-D)}, \tag{44}$$

$$\hat{y}\cdot\bar{\bar{\tilde{G}}}_{H2M}\cdot\hat{x}=\tilde{G}_{H_y2M_x}(k_x,k_y)=\frac{(k_xk_y)}{\varphi_2\omega\mu_0}e^{-j\varphi_2(z-D)}, \tag{45}$$

$$\hat{x}\cdot\bar{\bar{\tilde{G}}}_{H2M}\cdot\hat{y}=\tilde{G}_{H_x2M_y}(k_x,k_y)=\tilde{G}_{H_y2M_x}(k_y,k_x), \tag{46}$$

$$\hat{y}\cdot\bar{\bar{\tilde{G}}}_{H2M}\cdot\hat{y}=\tilde{G}_{H_y2M_y}(k_x,k_y)=\tilde{G}_{H_x2M_x}(k_y,k_x), \tag{47}$$

$$\hat{x}\cdot\bar{\bar{\tilde{G}}}_{H1M}\cdot\hat{x}=\tilde{G}_{H_x1M_x}(k_x,k_y)=\frac{j(k_0^2\epsilon_r-k_x^2)}{\varphi_1\omega\mu_0}\frac{\cos(\varphi_1 z)}{\sin(\varphi_1 D)}, \tag{48}$$

$$\hat{y}\cdot\bar{\bar{\tilde{G}}}_{H1M}\cdot\hat{x}=\tilde{G}_{H_y1M_x}(k_x,k_y)=\frac{-jk_xk_y}{\varphi_1\omega\mu_0}\frac{\cos(\varphi_1 z)}{\sin(\varphi_1 D)}, \tag{49}$$

$$\hat{x}\cdot\bar{\bar{\tilde{G}}}_{H1M}\cdot\hat{y}=\tilde{G}_{H_x1M_y}(k_x,k_y)=\tilde{G}_{H_y1M_x}(k_y,k_x), \tag{50}$$

$$\hat{y}\cdot\bar{\bar{\tilde{G}}}_{H1M}\cdot\hat{y}=\tilde{G}_{H_y1M_y}(k_x,k_y)=\tilde{G}_{H_x1M_x}(k_y,k_x), \tag{51}$$

$$\hat{z}\cdot\bar{\bar{\tilde{G}}}_{E2M}\cdot\hat{x}=\tilde{G}_{E_z2M_x}(k_x,k_y)=\frac{k_y}{\varphi_2}e^{-j\varphi_2(z-D)}, \tag{52}$$

$$\hat{z}\cdot\bar{\bar{\tilde{G}}}_{E2M}\cdot\hat{y}=\tilde{G}_{E_z2M_y}(k_x,k_y)=\frac{-k_x}{\varphi_2}e^{-j\varphi_2(z-D)}=-\tilde{G}_{E_z2M_x}(k_y,k_x), \tag{53}$$

$$\hat{z}\cdot\bar{\bar{\tilde{G}}}_{E1M}\cdot\hat{x}=\tilde{G}_{E_z1M_x}(k_x,k_y)=\frac{-jk_y\cos(\varphi_1 z)}{\varphi_1\sin(\varphi_1 D)}, \tag{54}$$

$$\hat{z}\cdot\bar{\bar{\tilde{G}}}_{E1M}\cdot\hat{y}=\tilde{G}_{E_z1M_y}(k_x,k_y)=-\tilde{G}_{E_z1M_x}(k_y,k_x)=\frac{jk_x\cos[\varphi_1(z-D)]}{\varphi_1\sin(\varphi_1 D)} \tag{55}$$

where

$$\varphi_2=\sqrt{k_0^2-k_x^2-k_y^2};\ \mathrm{Im}(\varphi_2)<0, \tag{56}$$

$$\varphi_1=\sqrt{k_0^2\epsilon_r-k_x^2-k_y^2}. \tag{57}$$

For all Green's function components, the subscript E or H stands for the electric or the magnetic field, respectively, the subscript M for the equivalent magnetic current (slot field) source, and the subscript 1 or 2 for the field location below or above the slot, respectively (see Figs. 1 and 2).

References

[1] H. Shigesawa, M. Tsuji, and A. A. Oliner, "Conductor backed slotline and coplanar waveguide: Dangers and fullwave analyses," in *IEEE Microwave Theory Tech Symp. Dig.*, 1988, pp. 199–202.

[2] ——, "Dominant mode leakage from printed circuit waveguides," *Radio Sci.*, vol. 26, no. 2, pp. 559–564, March–April 1991.

[3] N. K. Das and D. M. Pozar, "Full-wave spectral-domain computation of material radiation and guided wave losses in infinite multilayered printed transmission lines," *IEEE Trans. Microwave Theory Tech.*, vol. 39, no. 1, pp. 54–63, Jan. 1991

[4] D. S. Phatak, N. K. Das, and A. P. Defonzo, "Dispersion characteristics of optically excited coplanar striplines: Comprehensive full-wave analysis," *IEEE Trans. Microwave Theory Tech.*, vol. 38, no. 11, pp. 1719–1731, Nov. 1990.

[5] L. Carin and N. K. Das, "Leaky waves in broadside-coupled microstrips," *IEEE Trans Microwave Theory Tech*, vol. 40, no. 1, pp. 58–66, Jan. 1992.

[6] J. T. Williams, N. Nghiem, and D. R. Jackson, "Proper and improper modal solutions for inhomogeneous stripline," in *IEEE Microwave Theory Tech. Soc. Symp. Dig.*, 1991, pp. 567–570.

[7] M. Tsuji, H. Shigesawa, and A. Oliner, "New interesting leakage behavior on coplanar waveguides of finite and infinite widths," *IEEE Trans. Microwave Theory and Tech*, vol. 39, no. 12, pp 2130–2137, Dec. 1991.

[8] N. K. Das and D. M. Pozar, "Multiport scattering analysis of multilayered printed antennas fed by multiple feed ports, part I Theory; Part II: Applications," *IEEE Trans. Antennas Propagat*, vol. 40, no. 5, pp. 469–491, May 1992.

[9] T. Itoh, "Spectral domain immitance approach for dispersion characteristics of generalized printed transmission lines," *IEEE Trans. Microwave Theory Tech.,* vol. 28, no. 7, pp. 733–736, July 1980.
[10] J. B. Davies and D. Mirshekar-Syahkal, "Spectral domain solution of arbitrary coplanar transmission line with multilayer substrates," *IEEE Trans. Microwave Theory Tech.*, vol. MTT-25, no. 2, pp. 143–146, Feb. 1977.
[11] N. K. Das and D. M. Pozar, "A generalized spectral-domain Green's function for multilayer dielectric substrates with applications to multilayer transmission lines," *IEEE Trans. Microwave Theory Tech.,* vol. 35, no. 3, pp. 326–335, Mar. 1987.
[12] N. K. Das, "A Study of Multilayered Printed Antenna Structures," Ph.D. thesis, Dept. of Electrical and Computer Eng., Univ. of Massachusetts, Amherst, Sept. 1987.
[13] ——, "Power leakage, characteristic impedance and mode-coupling behavior of finite-length leaky printed transmission lines," *IEEE Trans. Microwave Theory Tech.,* 1996, to appear.
[14] R. W. Jackson, "Mode conversion at discontinuities in finite-width conductor-backed co-planar waveguide," *IEEE Trans. Microwave Theory Tech.*, vol. 37, no. 10, pp. 1582–1589, Oct. 1989.
[15] N. K. Das, "Characteristics of modified slotline configurations," in *IEEE Microwave Theory Tech. Symp. Dig.,* 1991, pp. 777–780.
[16] Y. Liu and T. Itoh, "Leakage phenomena in multilayered conductor-backed coplanar waveguides," *IEEE Microwave Guided Wave Lett.,* vol. 39, no. 11, pp. 426–427, Nov. 1993.

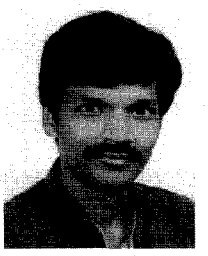

Nirod K. Das (S'89–M'89) was born in Puri, Orissa state, India, on February 27, 1963. He received the B.Tech(Hons.) degree in electronics and electrical communication engineering from the Indian Institute of Technology (IIT), Kharagpur, India, in 1985, and the M.S. and Ph.D. degrees in electrical engineering from the University of Massachusetts, Amherst, in 1987 and 1989, respectively.

From 1985 to 1989 he was with the Department of Electrical and Computer Engineering at the University of Massachusetts, Amherst, first as a Graduate Research Assistant and then, after receiving the Ph.D. degree, as a Postdoctoral Research Associate. In 1990 he joined the Department of Electrical Engineering at Polytechnic University, Farmingdale, NY, as an Assistant Professor. His research interests are in the general areas of microwave, millimeter wave, and optoelectronic integrated circuits and antennas, and in particular the analytical and experimental study of multiple layered structures for integrated circuit and phased array appplications.

Dr. Das has received a student prize paper award from the US National Council of URSI, and the 1992 R.W.P. King Best Paper Award from the Antennas and Propagation Society of IEEE, for his multilayer printed antenna work.